J. Bacteriol.

Regulatory small RNA, Qrr2, is expressed independently of sigma factor-54 and functions autonomously in *Vibrio parahaemolyticus* to control quorum sensing

Tague, J.G., J. Hong, S.S. Kalburge, and E.F. Boyd*

Department of Biological Sciences, University of Delaware, Newark, DE, 19716

Corresponding author*

Dr. E. Fidelma Boyd

Department of Biological Sciences

University of Delaware

Newark, DE 19716

Phone: (302) 831-1088. Fax: (302) 831-2281 Email: fboyd@udel.edu

Abstract

Bacterial cells alter gene expression in response to changes in population density in a process called quorum sensing (QS). In *Vibrio harveyi*, LuxO, a low cell density activator of sigma factor-54 (RpoN), is required for transcription of five non-coding regulatory sRNAs, Qrr1-Qrr5, which each repress translation of the master QS regulator LuxR. *Vibrio parahaemolyticus*, the leading cause of bacterial seafood-borne gastroenteritis, also contains five Qrr sRNAs that control OpaR (the LuxR homolog), required for capsule polysaccharide (CPS) and biofilm production, motility, and metabolism. We show that in a Δ*luxO* deletion mutant, *opaR* was de-repressed and CPS and biofilm were produced. However, in a Δ*rpoN* mutant, *opaR* was repressed, no CPS was produced, and less biofilm production was observed compared to wild type. To determine why *opaR* was repressed, expression analysis in Δ*luxO* showed all five *qrr* genes were repressed, while in Δ*rpoN* the *qrr2* gene was significantly de-repressed. Reporter assays and mutant analysis showed Qrr2 sRNA can act autonomously to control OpaR. Bioinformatics analysis identified a sigma-70 (RpoD) -35 -10 promoter overlapping the canonical sigma-54 (RpoN) promoter in the *qrr2* regulatory region. Mutagenesis of the sigma-70 -10 promoter site in the Δ*rpoN* mutant background, resulted in repression of *qrr2*. Analysis of *qrr* quadruple deletion mutants, in which only a single *qrr* gene is present, showed that only Qrr2 sRNA can act autonomously to regulate *opaR*. Mutant and expression data also demonstrated that RpoN and the global regulator Fis act

additively to repress *qrr2*. Our data has uncovered a new mechanism of *qrr* expression and shows that Qrr2 sRNA is sufficient for OpaR regulation.

Importance

The quorum sensing non-coding sRNAs are present in all *Vibrio* species but vary in number and regulatory roles among species. In the Harveyi clade, all species contain five *qrr* genes that, in *V. harveyi*, are additive in function to control LuxR. In the Cholerae clade, four *qrr* genes are present, and in *V. cholerae* the *qrr* genes are redundant in function to control HapR (the LuxR homolog). Here, we show that in *V. parahaemolyticus*, only *qrr2* can function autonomously to control OpaR, and it is controlled by two overlapping promoters. The *qrr2* sigma-70 promoter is present in all strains of *V. parahaemolyticus* and in other members of the Harveyi clade suggesting a conserved mechanism of regulation.

Introduction

Bacteria monitor changes in cell density using a process termed quorum sensing (QS) (1, 2). QS is a regulatory mechanism used to alter global gene expression in response to cell density changes (1-6). In many Gram-negative bacteria, N-acylhomoserine lactone (AHL) is a common QS autoinducer synthesized intracellularly and secreted out of the cell (2, 7). By surveying AHL levels in its environment, a bacterium can regulate gene expression in response to growth phase. Quorum sensing has been characterized in several marine species in the genus *Vibrio*, including *V. anguillarum, V. cholerae, V. harveyi* and *V. parahaemolyticus*, and shown to modulate expression of bioluminescence, capsule formation, biofilm, natural competence, swarming motility, and virulence (5, 7-21). In *V. harveyi* and *V. anguillarum*, it was shown that LuxO, the QS response regulator, is an activator of sigma factor-54, encoded by *rpoN* that along with RNA polymerase, initiates transcription of the non-coding quorum regulatory small RNAs (Qrr) (8, 22-23).

Non-coding sRNAs are a group of regulators present in prokaryotes that together with the RNA chaperone Hfq control gene expression in a range of phenotypes (24-26). The Qrr sRNAs are classified as *trans*-acting sRNAs that along with Hfq, target mRNA via base-pairing to the 5′ UTR to stabilize or destabilize translation. In *V. harveyi,* the nucleoid structuring protein Fis was shown to be a positive regulator of *qrr* gene expression (27). The Qrr sRNAs are post-transcriptional regulators that, in *V. harveyi*, enhanced translation of the QS low cell density (LCD) master regulator AphA and

inhibited translation of the QS high cell density (HCD) master regulator LuxR (28-31). At HCD in *V. harveyi*, LuxO is not phosphorylated and therefore cannot activate sigma-54 (RpoN), the five Qrr sRNA genes *qrr1* to *qrr5* are not transcribed, and LuxR translation is de-repressed. In addition, AphA and LuxR repress each other transcriptionally, providing a further level of regulation (30, 32-34). Studies have shown that in *V. harveyi*, Qrr1 has a 9-bp deletion in the 5′ region of the sRNA and therefore cannot activate *aphA* translation but can still repress *luxR* translation. The deletion in *qrr1* is also present in *V. cholerae, V. parahaemolyticus* and several other *Vibrio* species (30, 35). In *V. harveyi*, Qrr2, Qrr3, Qrr4, and Qrr5 sRNAs were additive in function and controlled the same target sites (29, 36, 37). However, the *qrr* genes showed distinct expression patterns and controlled the QS output signal at different levels coordinated with highest to lowest expression: Qrr4 > Qrr2 > Qrr3 > Qrr1 > Qrr5 (29). *V. cholerae* encodes four Qrr sRNAs, Qrr1 to Qrr4 that were redundant in function with any one of the four Qrr sRNAs sufficient to repress HapR (the LuxR homolog) (37).

Vibrio parahaemolyticus (VP) is a halophile, residing in marine environments as free-living organisms or in association with marine flora and fauna (38-40). This species is the leading cause of seafood-borne bacterial gastroenteritis worldwide, causing increasing infections each year, and is also a serious pathogen in the aquaculture industry (41, 42). *Vibrio parahaemolyticus* has dual flagellar systems, with the lateral flagellum system required for swarming motility, an important multicellular behavior

(43). *Vibrio parahaemolyticus* has the same QS components and pathway as *V. harveyi*, containing five Qrr sRNAs that are predicted to control *aphA* and *luxR* (Fig. 1). In this species, the LuxR homolog is named OpaR (Opacity Regulator), for its role as an activator of capsule polysaccharide (CPS) production that results in an opaque, rugose colony morphology (44). A Δ*opaR* mutant has a translucent, smooth colony morphology and does not produce CPS nor a robust biofilm (14, 16, 44, 45). Besides CPS and biofilm formation, OpaR has also been shown to regulate swimming and swarming motility, surface sensing, metabolism, and the osmotic stress response in this species (14, 15, 20, 46-49). A *V. parahaemolyticus* Δ*luxO* deletion mutant, in which the *qrr* sRNAs were not expressed, showed *opaR* was highly induced and produced both CPS and biofilm, output signals of the QS pathway (14). Interestingly, an earlier study examining an Δ*rpoN* deletion mutant in *V. parahaemolyticus* showed that it did not produce CPS nor biofilm (50). This is unexpected because previous studies in *V. harveyi* suggest that in a Δ*rpoN* mutant the *qrr* sRNA would not be expressed and therefore *luxR* (*opaR*) would be de-repressed and production of CPS and biofilm would be observed.

Here, we examined mutants of the QS pathway in *V. parahaemolyticus* to determine why the QS pathway output phenotypes differ between the Δ*luxO* and Δ*rpoN* mutants. We examined single and double mutants of Δ*luxO* and Δ*rpoN* for CPS and biofilm formation. We demonstrate that the Δ*luxO* mutant produces CPS and biofilm, whereas the Δ*rpoN* and Δ*rpoN*/Δ*luxO* mutants do not, suggesting *opaR* is repressed. We

113 determined the expression patterns of *opaR, aphA* and the five *qrr* genes in these
114 mutants and from this data, we determined that *qrr2* was de-repressed in the Δ*rpoN*
115 mutant and *opaR* was repressed. Deletion of *qrr2* in the Δ*rpoN* mutant background
116 resulted in *opaR* expression and restored CPS and biofilm production, demonstrating
117 that Qrr2 sRNA is responsible for the Δ*rpoN* mutant CPS defect phenotype.
118 Bioinformatics analysis of the *qrr2* regulatory region identified an RpoD-35 -10
119 promoter region that overlaps with the RpoN -24 -12 promoter suggesting a mechanism
120 by which *qrr2* is expressed in the *rpoN* mutant. We performed mutagenesis of the
121 putative -10 promoter site and showed that *qrr2* expression was repressed indicting that
122 *qrr2* can be transcribed from this promoter. To determine whether the other Qrr sRNAs
123 can also function independently, we constructed quadruple *qrr* mutants, in which only
124 one *qrr* is present, and examined CPS and motility phenotypes. Only the quad mutant
125 containing *qrr2* could recapitulate wild type phenotypes, indicating that it can act
126 autonomously to regulate OpaR. Furthermore, in a sigma-54 and Fis double mutant
127 (Δ*rpoN*/Δ*fis*), *qrr2* was more highly expressed than in a single Δ*rpoN* mutant, suggesting
128 that both RpoN and Fis act together to repress *qrr2* transcription by sigma-70. Sequence
129 comparative analysis showed that -35 and -10 promoter sites were conserved among
130 species within the Harveyi clade. Overall, our data show that Qrr2 can function
131 independently and has a novel mechanism of expression in *V. parahaemolyticus*.
132 **Results:**

Differential expression of *opaR* and *aphA* in Δ*luxO* versus Δ*rpoN* mutants. We used CPS production as a readout of OpaR presence in the *V. parahaemolyticus* cell. Based on the quorum sensing pathway in *V. harveyi*, we would expect both a Δ*luxO* and Δ*rpoN* deletion mutant to produce CPS, as the Qrr sRNAs should not be transcribed, and therefore OpaR should be de-repressed (**Fig. 1**). In a CPS assay, the Δ*luxO* mutant produced CPS forming opaque, rugose colonies. However, the Δ*rpoN* mutant did not produce CPS, instead forming a translucent, smooth colony morphology, similar to the Δ*opaR* strain (**Fig. 2A**). In addition, a Δ*rpoN*/Δ*luxO* double mutant also lacked CPS and produced a translucent, smooth colony morphology. Similarly, when we examined biofilm formation, both the Δ*rpoN* and Δ*rpoN*/Δ*luxO* double mutant strains produced less biofilm than the wild type and Δ*luxO* strains (**Fig. 2B**). These data suggest that in the Δ*rpoN* mutant, *opaR* is repressed. To test this, we complemented the Δ*rpoN* mutant with the *opaR* gene expressed from an arabinose promoter (pBAD*opaR*), and in these cells CPS production was restored, indicating that the absence of *opaR* in the Δ*rpoN* mutant led to the CPS defect (**Fig. S1**).

Next, we investigated the expression profiles of the QS master regulators in the Δ*luxO* and Δ*rpoN* deletion mutants. RNA isolation and quantitative real-time PCR (qPCR) assays were performed from cells grown in LB 3% NaCl to optical densities (OD) 0.1 and 0.5. At OD 0.1, expression of *opaR* in Δ*luxO* relative to wild type was significantly upregulated, however, *opaR* expression was unchanged in the Δ*rpoN*

mutant (**Fig. 3A**). At OD 0.5, expression of *opaR* in Δ*luxO* matched that of wild type, however, in the Δ*rpoN* mutant expression of *opaR* was significantly downregulated relative to wild type (**Fig. 3B**). Expression of *aphA*, the low cell density QS master regulator, was repressed in the Δ*luxO* mutant compared to wild type and unchanged in the Δ*rpoN* mutant at OD 0.1 (**Fig. 3C**). At OD 0.5, *aphA* expression was upregulated compared to wild type in Δ*rpoN* (**Fig. 3D**). These data indicate that *opaR* is repressed in the Δ*rpoN* deletion mutant.

Expression analysis of *qrr1-qrr5* in Δ*luxO* and Δ*rpoN* mutants. Since *opaR* showed different levels of expression in the Δ*luxO* and Δ*rpoN* deletion mutants, we wanted to determine whether this was due to differences in *qrr* expression levels. We examined expression of all five *qrr* genes in cells grown to OD 0.1 and OD 0.5 and show that the expression of *qrr1, qrr2, qrr3* and *qrr5* was higher at OD 0.1 relative to OD 0.5 (**Fig. S2)**. Expression of *qrr4* was detected at OD 0.1 but was not detected at OD 0.5 in wild type. In addition, *qrr4* expression was not detected in either Δ*luxO* or Δ*rpoN* at OD 0.1 or 0.5. Next, we examined expression of the *qrr* genes at OD 0.1 in the Δ*luxO* mutant relative to wild type and showed *qrr1* expression was unchanged and there was significant downregulation of *qrr2, qrr3,* and *qrr5* (**Fig 4A**). Whereas at OD 0.5, their expression matched that of wild type (**Fig. 4B**). In the Δ*rpoN* mutant, expression of *qrr1, qrr3*, and *qrr5* matched that of the Δ*luxO* mutant (**Fig. 4C**), however, *qrr2* was upregulated at both OD 0.1 and OD 0.5 (**Fig. 4D**). To confirm that *qrr2* was differentially regulated between

173 Δ*luxO* and Δ*rpoN*, the *qrr2* regulatory region was cloned into pRU1064 reporter vector
174 upstream of a promoter-less *gfp* cassette (P*qrr2-gfp*). The specific fluorescence of P*qrr2-*
175 *gfp* was examined in the wild type, Δ*luxO,* and Δ*rpoN* mutants and measured as a
176 cumulative read-out of *qrr2* transcription (**Fig. 5A**). The level of specific fluorescence of
177 P*qrr2-gfp* was reduced in the Δ*luxO* mutant relative to wild type, whereas in the Δ*rpoN*
178 mutant, fluorescence was significantly increased (**Fig. 5A**). Next, we examined the *opaR*
179 regulatory region cloned into pRU1064 reporter vector upstream of a promoter-less *gfp*
180 cassette (P*opaR-gfp*) in wild type, a Δ*qrr2* single mutant and a Δ*qrr3,1,4,5* quadruple
181 mutant with only *qrr2* present (**Fig. 5B**). In Δ*qrr2* compared to wild type, P*opaR-gfp*
182 showed significantly increased fluorescence, whereas the quadruple *qrr* deletion
183 mutant, with *qrr2* present, was similar to wild type (**Fig. 5B**). We predicted that deletion
184 of *qrr2* in the Δ*rpoN* mutant background should restore *opaR* expression and CPS
185 production. We constructed a Δ*rpoN*/Δ*qrr2* double mutant and examined *opaR* and *aphA*
186 expression levels (**Fig. S3)**. Quantitative real time PCR assays showed that *opaR* was
187 highly expressed in a Δ*rpoN*/Δ*qrr2* double mutant compared to wild type (**Fig. S3**).
188 Examination of CPS formation showed that the Δ*rpoN*/Δ*qrr2* double mutant produced a
189 rough colony morphology (**Fig. S4A**). Similarly, in biofilm assays, the Δ*rpoN* mutant
190 produced a significantly reduced biofilm, whereas the Δ*rpoN*/Δ*qrr2* double mutant
191 produced a biofilm similar to wild type (**Fig. S4B**). Overall, these data demonstrate that

Qrr2 sRNA is present in the Δ*rpoN* deletion mutant and Qrr2 sRNA can function autonomously to control OpaR and QS phenotypes.

Overlapping sigma-70 and sigma-54 promoters. The expression of *qrr2* in the Δ*rpoN* mutant background indicates that an additional sigma factor can initiate *qrr2* transcription. To examine this further, the regulatory regions of *qrr1* to *qrr5* in *V. parahaemolyticus* RIMD2210633 were aligned and, using bioinformatics tools, surveyed for the presence of promoter regions. Although the five Qrr sRNAs share homology, their regulatory regions are divergent with the exception of the sigma-54 canonical -24 (T**TGGC**A) and -12 (AAT**GCA**) promoter sites, with nucleotides in bold conserved amongst all five *qrr* regulatory regions (**Fig. S5**). In the regulatory region of *qrr2*, promoter analysis identified a housekeeping sigma-70 (RpoD) -35 (TTGAAA) and -10 (ATAATA) promoter (**Fig. 6A**). The putative sigma-70 promoter overlapped with the sigma-54 -24 and -12 promoter (**Fig. 6A**), and was absent from the regulatory regions of *qrr1*, *qrr3*, *qrr4*, and *qrr5* (**Fig. S5**). This suggested that *qrr2* can be transcribed by either sigma-54 or sigma-70 and could explain its expression in the absence of *rpoN*. To examine this further, we mutated three base-pairs of the putative sigma-70 -10 ATAATA site to ATACCC in the pRUP*qrr2* reporter vector (**Fig. 6A**). The mutagenized vector, pRUP*qrr2*-10CCC, was conjugated into wild type and Δ*rpoN* and specific fluorescence was determined. The Δ*rpoN* pRUP*qrr2*-10CCC strain showed significantly reduced fluorescence relative to Δ*rpoN* pRUP*qrr2*, indicating that this site is required for

qrr2 transcription in the absence of RpoN (**Fig. 6B**). The data suggests that *qrr2* can be transcribed by two sigma factors using dual overlapping promoters, suggesting a unique mode of regulation for Qrr2 sRNA. Comparisons of the *qrr2* regulatory region among Harveyi clade species *V. alginolyticus, V. campbellii, V. harveyi,* and *V. parahaemolyticus* showed that the sigma-70 promoter -10 region was highly conserved among these species (**Fig. S6**). Each of the five Qrr sRNAs also shared homology among these species (**Fig. S7**). The *qrr1* gene among all four species showed high homology clustering closely together on the phylogenetic tree, but were distantly related to the other four *qrr* genes. The *qrr3* and *qrr4* genes each clustered tightly together on the tree whereas *qrr2* and *qrr5* each showed divergence among the species (**Fig. S7**). Overall divergence in regulatory regions and gene sequence amongst the *qrr* genes likely suggests differences in how each *qrr* gene is regulated and differences in the target genes of each Qrr sRNA.

Qrr2 sRNA can function autonomously. Next, we determined whether Qrr2 sRNA has a distinct role in this species and whether any of the four other *qrr* genes can act independently. Using a *qrr1-qrr5* quintuple deletion mutant (Δ*qrr*-null) and five quadruple *qrr* deletion mutants, each containing a single *qrr*, we examined several QS phenotypes (**Fig. S8**). In swarming motility assays, the Δ*qrr*-null strain was swarming deficient, as swarming is negatively regulated by OpaR **(Fig. S8A)**. In addition, four quadruple mutants, Δ *qrr3,2,4,5;* Δ*qrr2,1,4,5;* Δ*qrr3,2,1,5;* and Δ*qrr3,2,1,4* were all

swarming deficient indicating that Qrr1, Qrr3, Qrr4 and Qrr5 sRNAs cannot function independently to control this phenotype (**Fig. S8A)**. In swarming motility assays, the Δ*qrr3,1,4,5* mutant that contained only *qrr2*, behaved similar to wild type and was swarming proficient **(Fig. S8A)**. In swimming assays, the quad mutants that lacked *qrr2* produced similar results to the null mutant with defects in swimming (**Fig. S8B)**. Whereas only Δ*qrr3,1,4,5* that contains only *qrr2* showed swimming motility similar to wild type (**Fig. S8B**). Additionally, in CPS assays the *qrr2* positive strain also showed a colony morphology similar to wild type (**Fig. S8C**). Analysis of a single *qrr2* deletion mutant indicates that it is not essential for CPS production or swarming and that the other *qrr* genes can function in the absence of *qrr2* (**Fig. S9**). In summary, these data demonstrate that only Qrr2 sRNA can function independently in *V. parahaemolyticus*.

RpoN and Fis are not required for *qrr2* expression. In order to identify additional regulators of *qrr2* transcription, a DNA-affinity pull-down was performed. We used Δ*rpoN* cell lysate grown to OD 0.5 and P*qrr2* bait DNA. We identified a number of candidate regulators previously shown to bind to the *qrr* sRNA regulatory regions in *V. harveyi* (27, 34, 51) (**Fig. S10 and S11**). We decided to examine the nucleoid associated protein Fis further since it is known to be a positive regulator of *qrr* sRNA expression and binds to the *qrr* sRNA regulatory regions in *V. harveyi* (27). We identified three putative Fis binding sites in the *qrr2* regulatory region using virtual footprint analysis based off the E. coli Fis consensus sequence. A Fis binding site was located adjacent to

the -35 promoter site, as well as two additional Fis binding sites, at 193-bp and 229-bp upstream of the *qrr2* transcriptional start site (**Fig. 7A**). To confirm these Fis binding sites, we constructed four DNA probes of the *qrr2* regulatory region to use in electrophoretic shift mobility assays (EMSAs) with purified Fis protein. DNA probe 1 encompassed the entire *qrr2* regulatory region and showed Fis binding in a concentration dependent manner via EMSA (**Fig 7B**). DNA probe 1A encompassing the single binding site showed binding in a concentration dependent manner, and similarly Fis bound to probe 1C which contained the two putative sites **(Fig. 7B**). Probe 1B, which did not have a putative Fis binding site, showed non-specific binding. Next, we examined expression of the P*qrr2-gfp* reporter in wild type, Δ*rpoN* and a Δ*rpoN*/Δ*fis* double mutant and confirmed that expression of P*qrr2-gfp* was upregulated in the Δ*rpoN* mutant but was even more highly upregulated in the Δ*rpoN*/Δ*fis* double mutant (**Fig. 7C**). These data indicate that both Fis and RpoN can act as repressors of *qrr2* in *V. parahaemolyticus*, and Fis likely plays a role in enhancing sigma-54 binding.

Discussion

In this study, we investigated the role of sigma-54, LuxO, and the five Qrr sRNAs in the *V. parahaemolyticus* QS pathway and showed that sigma-54, *qrr1, qrr3, qrr4,* and *qrr5* were not essential components. Our data demonstrated that in a Δ*rpoN* mutant, cells had a defect in CPS and biofilm formation, QS phenotypes that differed from the Δ*luxO* mutant. The data showed that Qrr2 is highly expressed in a Δ*rpoN* mutant and that Qrr2

can act autonomously to repress OpaR expression and QS phenotypes. In a Δ*rpoN*/Δ*qrr2* double mutant, *opaR* was de-repressed and CPS and biofilm formation were restored. Bioinformatics analysis identified a putative -35 -10 promoter region within the *qrr2* regulatory region and mutagenesis of the -10 promoter sites resulted in repression of *qrr2*. Overall, the data indicate that *qrr2* can be expressed from two promoters, which is unique to *qrr2* in *V. parahaemolyticus,* but is likely true of related species. There have been other accounts of sigma-54-dependent genes showing increased transcription in the absence of *rpoN* (52, 53). In these cases, a putative sigma-70 promoter was present, suggesting a potential competition for promoter sites (52, 53). For example, in *E. coli, glmY* a coding sRNA contained overlapping sigma-54 and sigma-70 promoters, which were shown to allow for precise control of *glmY* expression within the cell (54). In our study, we identified a sigma-70 promoter that overlaps with the sigma-54 consensus promoter sequence of *qrr2*, suggesting that RpoN under differ growth conditions may block RpoD access. We propose that in the wild type background, *qrr2* is transcribed via LuxO activated RpoN, and in the Δ*luxO* mutant, *qrr2* is not transcribed because sigma-54 is in an inactive state bound to the *qrr2* promoter, physically blocking additional sigma factors from binding. However, in the absence of sigma-54, sigma-70 is able to bind to the *qrr2* regulatory region at a conserved -35 and -10 region to initiate transcription (**Fig. 8**). Fis is a global regulator that is known to enhance and inhibit transcription from promoter regions in many bacterial species (55-58). In *V. harveyi*, Fis

has been shown to positively regulate *qrr* expression (27). Here, we show in DNA protein binding assays in *V. parahaemolyticus* that Fis binds adjacent to the -35 promoter site. We speculate that Fis functions to enhance RpoN promoter binding to maximize *qrr* expression. The data showed that in the absence of both RpoN and Fis, however, *qrr2* expression is significantly increased compared to the Δ*rpoN* mutant alone. Under these conditions additional binding sites within the *qrr2* regulatory region may be fully exposed, allowing sigma-70 full access for increased *qrr2* expression (**Fig. 8)**. A study in *V. alginolyticus* MVP01, a species closely related to *V. parahaemolyticus*, also showed differences between the Δ*luxO* and Δ*rpoN* mutant strains in their control of cell density dependent siderophore production. The Δ*luxO* mutant showed reduced siderophore production, which is negatively regulated by LuxR, and the Δ*rpoN* mutant showed increased production (59). Their data showed RpoN dependent and independent siderophore production. We speculate that this could be the result of expression by RpoD since *V. alginolyticus* has a -35 -10 promoter in the Qrr2 regulatory region (**Fig. S6**).

In *V. cholerae*, four Qrr sRNAs (Qrr1-Qrr4) are present that were shown to act redundantly to control bioluminescence, that is, any one of the Qrr sRNAs is sufficient to control HapR (LuxR homolog) (37). In their study, Lenz and colleagues showed that it was not until all four Qrrs were deleted in *V. cholerae*, that there is a difference in density-dependent bioluminescence (37). In *V. harveyi*, the five Qrrs were shown to act

312 additively to control LuxR expression. Using bioluminescence assays and quadruple *qrr*
313 mutants, it was determined that each Qrr has a different level of strength in repressing
314 *luxR* translation (29). In our study in *V. parahaemolyticus*, the data showed that
315 expression of *qrr4* was restricted to low cell density cells and *qrr4* expression had an
316 absolute requirement for LuxO and RpoN. We demonstrated that Qrr2 sRNA is the
317 only Qrr that can act autonomously to control QS gene expression, but is not essential,
318 since a Δ*qrr2* mutant behaves like wild type (**Fig. S9**). Given that *qrr2* can be transcribed
319 independent of RpoN, we propose that Qrr2 may have unique functions and/or targets
320 in this species. We propose that *V. parahaemolyticus* can activate the transcription of *qrr2*
321 via RpoN or RpoD to timely alter gene expression likely under different growth
322 conditions.

323 **Materials and Methods:**

324 **Bacterial strains and media.** In this study, the wild type (WT) strain is a streptomycin-
325 resistant clinical isolate of *Vibrio parahaemolyticus* RIMD2210633 and all strains used are
326 described in **Table 1**. All *V. parahaemolyticus* strains were grown in lysogeny broth (LB;
327 Fisher Scientific, Fair Lawn, NJ) supplemented with 3% NaCl (LBS) (weight/volume). *E.*
328 *coli* strains were grown in LB 1% NaCl. A diaminopimelic acid (DAP) auxotroph of *E.*
329 *coli* β2155 *λpir* was grown with 0.3 mM DAP in LB 1% NaCl. All strains were grown
330 aerobically at 37°C. Antibiotics were used in the following concentrations:

chloramphenicol (Cm), 12.5 μg/mL, streptomycin (Str), 200 μg/mL; and tetracycline (Tet), 1 μg/mL.

Construction of *V. parahaemolyticus* mutants. We created the double deletion mutants Δ*rpoN*/Δ*luxO* and Δ*rpoN*/Δ*fis* using mutant vectors pDSΔ*luxO* and pDSΔ*fis,* conjugated into the *V. parahaemolyticus* Δ*rpoN* mutant background. The Δ*qrr*-null mutant was constructed by creating truncated, non-functional copies of each *qrr* using SOE primer design, with primers listed in **Table 2.** All truncated *qrr* products were cloned into pDS132 suicide vector, transformed into the *E. coli* β2155 *λpir*, followed by conjugation and homologous recombination into the *V. parahaemolyticus* genome. Positive single-cross over colonies were selected using Cm. To induce a double crossover event, a positive single-cross strain was grown overnight in the absence of Cm, leaving behind either the truncated *qrr* allele or the wild-type allele in the genome. The overnight culture was plated on sucrose plates for selection of normal versus soupy colony morphology, as the colonies still harboring the pDS132Δ*qrr* vector appear irregular due to the *sacB* gene. Colonies were screened via PCR for the truncated allele and sequenced to confirm deletion. The *qrr* null mutant was constructed by deleting qrr genes in the following order: *qrr3, qrr2, qrr1, qrr4, qrr5*. The quadruple Δ*qrr3*/Δ*qrr2*/Δ*qrr4*/Δ*qrr5* mutant was constructed by re-introducing *qrr1* into the Δ*qrr*-null mutant, and similarly *qrr2* and *qrr3* were each separately cloned into the Δ*qrr*-null mutant to create their corresponding quad mutants. The Δ*qrr3*/Δ*qrr2*/Δ*qrr1*/Δ*qrr5* mutant

was constructed by deleting *qrr5* in the Δ*qrr3*/Δ*qrr2*/Δ*qrr1* mutant background and Δ*qrr3*/Δ*qrr2*/Δ*qrr1*/Δ*qrr4* was constructed by knocking out *qrr4* in the Δ*qrr3*/Δ*qrr2*/Δ*qrr1* background. The Δ*qrr2* single mutant was constructed using the pDSΔ*qrr2* construct conjugated into the wild type background. The Δ*rpoN*/Δ*qrr2* mutant was constructed by conjugating the pDSΔ*qrr2* vector into the Δ*rpoN* background. All mutants were sequenced to confirm deletions or insertions, ensuring in-frame mutant strains.

RNA isolation and real-time PCR. *Vibrio parahaemolyticus* wild type and mutants were grown overnight in LBS. Cells were washed twice with 1x phosphate-buffered saline (PBS) and diluted 1:50 into a fresh 5 mL culture of LBS. Cells were harvested at 0.1 OD and 0.5 OD and pelleted at 4°C. RNA was isolated from 4 mL of culture using the miRNAeasy Mini Kit (Qiagen, Hilden, Germany) and Qiazol lysis reagent. The concentration and purity of RNA was determined using a NanoDrop spectrophotometer (Thermo Scientific, Waltham, MA). RNA was treated with Turbo DNase (Invitrogen) and cDNA was synthesized using Superscript IV reverse transcriptase (Invitrogen) from 500 ng of RNA by priming with random hexamers. cDNA was diluted 1:10 for quantitative real-time PCR (qPCR) run on an Applied Biosystems QuantStudio™ 6 fast real-time PCR system (Applied Biosystems, Foster City, CA) using PowerUp SYBR green master mix (Life Technologies). qPCR primers used to amplify *opaR, aphA, qrr1, qrr2, qrr3, qrr4, qrr*5, and *16S* rRNA are listed in **Table 2** for reference. Cycle thresholds (C_T) values were used to determine expression levels

normalized to 16S rRNA levels. Expression was calculated relative to wild-type 16S rRNA using the $\Delta\Delta C_T$ method (60).

Transcriptional GFP-reporter assay. The P*qrr2* reporter construct was created using the pRU1064 vector, which contains a promoter-less *gfp* cassette, as well as Tet and Amp resistance genes (61). Primers, listed in **Table 2**, were designed using NEBuilder online software to amplify the 337-bp regulatory region of *qrr2* from *V. parahaemolyticus* RIMD2210633 genomic DNA. The pRU1064 vector was purified, digested with Spe1, and ligated with the P*qrr2* fragment via Gibson assembly protocol (62). The plasmid was then transformed into β2155 *λpir* and subsequently conjugated into wild-type and Δ*luxO*, Δ*rpoN,* and Δ*rpoN*/Δ*fis* mutants. Cultures were grown overnight in LBS with 1μg/mL Tet, washed twice with 1xPBS and then diluted 1:1000 into fresh LBS + Tet and grown for 20 hours at 37°C. Cultures were washed twice with 1xPBS and loaded into a black, clear-bottom 96-well plate. Final OD and GFP relative fluoresces were determined using a Tecan Spark microplate reader with Magellan software with excitation at 385 nm and emission at 509 nm (Tecan Systems, Inc., San Jose, CA). Specific fluorescence was calculated by dividing the relative fluorescence by the final OD. This experiment was performed in three biological replicates.

Splicing by overlap extension (SOE) primer design was used to construct a mutated (ATA-10CCC) RpoD promoter. We used the same SOE*qrr2*A and SOE*qrr2*D primers used to construct the Δ*qrr2* mutant in order to create a mutated *qrr2* regulatory

region. In addition, SOE primers P*qrr2*SDMB and P*qrr2*SDMC (**Table 2**) have complementary overlapping sequences that amplify a mutated promoter, indicated in bold. Fragments AB and CD were then used as a template to amplify the AD fragment, containing a mutated RpoD -10 promoter. The AD fragment was then used as the template to create a fragment containing only the *qrr2* regulatory region (337-bp) using Gibson assembly primers P*qrr2*SDM_GAfwd and P*qrr2*SDM_GArev. This mutated regulatory region was then ligated with SpeI digested pRU1064 using Gibson assembly and confirm via sequencing.

Capsule polysaccharide (CPS) formation assay. Capsule polysaccharide (CPS) formation assays were conducted as previously described (14, 45). In brief, single colonies of wild type and QS mutants were grown on heart infusion (HI) (Remel, Lenexa, KS) plates containing 1.5% agar, 2.5 mM $CaCl_2$, and 0.25% Congo red dye for 48 h at 30°C. Each image is an example from at least three biological replicates. The pBAD33 expression vector was used to overexpress *opaR* in wild type and Δ*rpoN* backgrounds. The *opaR* coding region, plus 30-bp upstream to include the ribosomal binding site, were amplified from *V. parahaemolyticus* RIMD2210633 genome via Phusion High-Fidelity (HF) polymerase PCR (New England Biolabs). The amplified 670-bp *opaR* coding region and pBAD33 empty vector (pBADEV) were digested with XbaI and HindIII restriction enzymes prior to ligation and transformation into *E. coli* β2155. pBAD*opaR* and pBADEV were conjugated into wild type, Δ*rpoN,* and Δ*opaR,* and

411 plated on Congo red plates to observe CPS formation. For strains containing pBAD,
412 0.1% (wt/vol) arabinose and 5 μg/mL of Cm were added to the media after autoclaving,
413 to induce and maintain the plasmid, respectively.

414 **Biofilm assay.** *Vibrio parahaemolyticus* cultures were grown overnight in LBS at 37˚C
415 with shaking. The overnight cultures were then used to inoculate a 96-well plate in a
416 1:50 dilution with LBS. After static incubation at 37˚C for 24 h, the culture liquid was
417 removed and the wells were washed with 1xPBS. Crystal violet (Electron Microscopy
418 Sciences), at 0.1% w/v, was added to the wells and incubated for 30 min at room
419 temperature. The crystal violet was removed, and wells were washed twice with 1xPBS.
420 The adhered crystal violet was solubilized in DMSO for an optical density reading at
421 595nm (OD_{595}).

422 **Motility assays.** Swimming and swarming assays were performed as previously
423 described (14, 50). To assess swimming, a pipette tip was used to pick a single colony
424 and stab into the center of an LB plate containing 2% NaCl and 0.3% agar. Plates were
425 incubated for 24 h at 37°C. Three biological replicates were performed, and the diameter
426 of growth was measured for quantification. Swarming assays were conducted on HI
427 plates containing 2% NaCl and 1.5% agar and incubated at 30°C for 48 h before
428 imaging.

429 **DNA-affinity pull-down.** A DNA-affinity pull-down was performed using previously
430 described methods, with modifications as needed (63-65). Bait DNA primers were

designed to amplify the regulatory region of *qrr2* (346-bp) with a biotin moiety added to the 5′ end. In addition, a negative control bait DNA (VPA1624 coding region, 342-bp) was amplified. Both bait DNA probes were amplified using Phusion HF polymerase (New England Biolabs) PCR and purified using ethanol extraction techniques (66). A 5 mL overnight culture of Δ*rpoN* grown in LB 3% NaCl was used to inoculate a fresh 100 mL culture of LB 3% NaCl grown at 37˚C with aeration. The culture was pelleted at 0.5 OD at 4°C for 30 min and stored overnight at 80˚C. The cell pellet was suspended in 1.5 mL of Fastbreak lysis buffer (Promega, Madison, WI) and sonicated to shear genomic DNA. The Δ*rpoN* lysate was pre-cleared with streptavidin DynaBeads (Thermo Scientific, Waltham, MA) to remove non-specific protein-bead interactions. Beads were incubated with 200 µL of probe DNA for 20 min, twice. The Δ*rpoN* lysate and sheared salmon sperm DNA (10µg/mL), as competitive DNA, were incubated with the beads twice, and washed. Protein candidates were eluted from the bait DNA-bead complex using elution buffers containing increasing concentrations of NaCl (100mM, 200mM, 300mM, 500mM, 750mM and 1M). 6X SDS was added to samples along with 1mM β-mercaptoethanol (BME) and then boiled at 95˚C for 5 min. A total of 25 µL of each elution was run on 2 stain-free, 12% gels and visualized using the Pierce™ Silver Stain for Mass Spectrometry kit (Thermo Scientific, Waltham, MA). P*qrr2* bait and negative control bait were loaded next to each other in order of increasing NaCl concentrations. Bands present in the P*qrr2* bait lanes, but not in the negative control lanes were selected

and cut from the gel. Each fragment was digested separately with trypsin using standard procedures and prepared for Mass Spectrophotometry 18C ZipTips (Fisher Scientific, Fair Lawn, NJ). Candidates were eluted in 10 μL twice, pooled, and dried again using SpeedVac. Dried samples were analyzed using the Thermo Q-Exactive Orbitrap and analyzed using Proteome Discoverer 1.4.

Fis protein purification. Fis was purified using the method previously described (48). Briefly, primer pair FisFWDpMAL and FisREVpMAL was used to amplify *fis* (VP2885) from *V. parahaemolyticus* RIMD2210633. The *fis* gene was cloned into the pMAL-c5x expression vector fused to a 6X His tag maltose binding protein (MBP) separated by a tobacco etch virus (TEV) protease cleavage site. Expression of pMAL*fis* in *E. coli* BL21 (DE3) was induced with 0.5 mM IPTG once the culture reached 0.4 OD_{595} and grown overnight at room temperature. Cells were harvested, suspended in lysis buffer (50 mM NaPO4, 200 mM NaCl, and 20 mM imidazole buffer [pH 7.4]), and lysed using a microfluidizer. The lysed culture was run over an IMAC column using HisPur Ni-NTA resin, followed by additional washing steps. Mass spectrometry was performed to confirm Fis protein molecular weight and SDS-PAGE was conducted to determine its purity along with A260/280 ratio analysis using a Nano drop.

Electrophoretic mobility shift assay for Fis. Purified Fis was used to conduct EMSAs using conditions previously described (48). Briefly, 30 ng of DNA probe was incubated with various concentrations of Fis (0 to 1.94 μM) in binding buffer (10 mM Tris, 150 mM

KCL, 0.1 mM dithiothreitol, 0.1 mM EDTA, 5% PEG, pH7.4) for 20 min. The concentration of Fis was determined using Bradford reagent. A 6% native polyacrylamide gel was pre-run for 2 h at 4°C (200V) with 1x Tris-acetate-EDTA (TAE) buffer. The incubated DNA-protein samples were then loaded onto the gel (10 μL) and run for 2 h in the same conditions. The gel was stained in an ethidium bromide bath (0.5μg/mL) for 15 min before imaging. P*qrr2* was further divided into a smaller probe to determine specificity of Fis binding to P*qrr2*.

References

1. Fuqua WC, Winans SC, Greenberg EP. 1994. Quorum sensing in bacteria: the LuxR-LuxI family of cell density-responsive transcriptional regulators. J Bacteriol 176:269-75.

2. Swift S, Downie J, Whitehead N, Barnard A, Salmond G, P W. 2001. Quorum sensing as a population-density-dependent determinant of bacterial physiology. Adv Microb Physiol 45:199-270.

3. Gray KM, Passador L, Iglewski BH, Greenberg EP. 1994. Interchangeability and specificity of components from the quorum-sensing regulatory systems of Vibrio fischeri and Pseudomonas aeruginosa. J Bacteriol 176:3076-80.

4. Nealson KH, Platt T, Hastings JW. 1970. Cellular Control of the Synthesis and Activity of the Bacterial Luminescent System1. J Bacteriol 104:313-22.

5. Miller MB, Skorupski K, Lenz DH, Taylor RK, Bassler BL. 2002. Parallel quorum sensing systems converge to regulate virulence in Vibrio cholerae. Cell 110:303-14.

6. Miller MB, Bassler BL. 2001. Quorum sensing in bacteria. Annu Rev Microbiol 55:165-99.

7. Bassler BL, Greenberg EP, Stevens AM. 1997. Cross-species induction of luminescence in the quorum-sensing bacterium Vibrio harveyi. J Bacteriol 179:4043-5.

8. Lilley BN, Bassler BL. 2000. Regulation of quorum sensing in Vibrio harveyi by LuxO and sigma-54. Mol Microbiol 36:940-54.

9. Egland KA, Greenberg EP. 1999. Quorum sensing in Vibrio fischeri: elements of the luxl promoter. Mol Microbiol 31:1197-204.

10. Dunlap PV. 1999. Quorum regulation of luminescence in Vibrio fischeri. J Mol Microbiol Biotechnol 1:5-12.

11. Camara M, Hardman A, Williams P, Milton D. 2002. Quorum sensing in Vibrio cholerae, p 217-8, Nat Genet, vol 32, United States.

12. Zhu J, Miller MB, Vance RE, Dziejman M, Bassler BL, Mekalanos JJ. 2002. Quorum-sensing regulators control virulence gene expression in Vibrio cholerae. Proc Natl Acad Sci U S A 99:3129-34.

13. Bassler BL, Wright M, Showalter RE, Silverman MR. 1993. Intercellular signaling in Vibrio harveyi: sequence and function of genes regulating expression of luminescence. Mol Microbiol 4:773-86.

14. Kalburge SS, Carpenter MR, Rozovsky S, Boyd EF. 2017. Quorum Sensing Regulators Are Required for Metabolic Fitness in Vibrio parahaemolyticus. Infect Immun 85:930-16.

15. Kernell Burke A, Guthrie LTC, Modise T, Cormier G, Jensen RV, McCarter LL, Stevens AM. 2015. OpaR Controls a Network of Downstream Transcription Factors in Vibrio parahaemolyticus BB22OP, PLoS One, vol 10.

524 16. Zhang Y, Qiu Y, Tan Y, Guo Z, Yang R, Zhou D. 2012. Transcriptional regulation
525 of opaR, qrr2-4 and aphA by the master quorum-sensing regulator OpaR in
526 Vibrio parahaemolyticus. PLoS One 7:e34622.
527 17. Trimble MJ, McCarter LL. 2011. Bis-(3'-5')-cyclic dimeric GMP-linked quorum
528 sensing controls swarming in Vibrio parahaemolyticus. Proc Natl Acad Sci U S A
529 108:18079-84.
530 18. Sun F, Zhang Y, Wang L, Yan X, Tan Y, Guo Z, Qiu J, Yang R, Xia P, Zhou D.
531 2012. Molecular Characterization of Direct Target Genes and cis-Acting
532 Consensus Recognized by Quorum-Sensing Regulator AphA in Vibrio
533 parahaemolyticus. PLoS One 7:e44210.
534 19. Zhang Y, Zhang L, Hou S, Huang X, Sun F, Gao H. 2016. The Master Quorum-
535 Sensing Regulator OpaR is Activated Indirectly by H-NS in Vibrio
536 parahaemolyticus. Current microbiology 73:71-6.
537 20. Enos-Berlage JL, Guvener ZT, Keenan CE, McCarter LL. 2005. Genetic
538 determinants of biofilm development of opaque and translucent Vibrio
539 parahaemolyticus. Mol Microbiol 55:1160-82.
540 21. Ishikawa T, Rompikuntal P, Lindmark B, Milton D, Wai S. 2009. Quorum sensing
541 regulation of the two hcp alleles in Vibrio cholerae O1 strains. PloS One 4:e6734.
542 22. Weber B, Lindell K, El Qaidi S, Hjerde E, Willassen N, Milton D. 2011. The
543 phosphotransferase VanU represses expression of four qrr genes antagonizing

544 VanO-mediated quorum-sensing regulation in Vibrio anguillarum. Microbiology
545 157:3324-3339.
546 23. Weber B, Croxatto A, Chen C, Milton D. 2008. RpoS induces expression of the
547 Vibrio anguillarum quorum-sensing regulator VanT. Microbiology 154:767-780.
548 24. Waters LS, Storz G. 2009. Regulatory RNAs in Bacteria. Cell 136:615-28.
549 25. Storz G, Vogel J, Wassarman KM. 2011. Regulation by small RNAs in bacteria:
550 expanding frontiers. Mol Cell 43:880-91.
551 26. Updegrove T, Zhang A, Storz G. 2016. Hfq: the flexible RNA matchmaker. Curr
552 Opin Microbiol 30:133-138.
553 27. Lenz DH, Bassler BL. 2007. The small nucleoid protein Fis is involved in Vibrio
554 cholerae quorum sensing. Mol Microbiol 63:859-71.
555 28. Papenfort K, Bassler BL. 2016. Quorum sensing signal-response systems in
556 Gram-negative bacteria. Nat Rev Microbiol 14:576-88.
557 29. Tu KC, Bassler BL. 2007. Multiple small RNAs act additively to integrate sensory
558 information and control quorum sensing in Vibrio harveyi. Genes Dev 21:221-33.
559 30. Shao Y, Bassler BL. 2012. Quorum-sensing non-coding small RNAs use unique
560 pairing regions to differentially control mRNA targets. Mol Microbiol 83:599-611.
561 31. Svenningsen S. 2018. Small RNA-Based Regulation of Bacterial Quorum Sensing
562 and Biofilm Formation. Microbiol Spectr 6.

563 32. Lin W, Kovacikova G, Skorupski K. 2007. The quorum sensing regulator HapR
564 downregulates the expression of the virulence gene transcription factor AphA in
565 Vibrio cholerae by antagonizing Lrp- and VpsR-mediated activation. Mol
566 Microbiol 64:953-67.
567 33. Pompeani AJ, Irgon JJ, Berger MF, Bulyk ML, Wingreen NS, Bassler BL. 2008.
568 The Vibrio harveyi master quorum-sensing regulator, LuxR, a TetR-type protein
569 is both an activator and a repressor: DNA recognition and binding specificity at
570 target promoters. Mol Microbiol 70:76-88.
571 34. Rutherford ST, van Kessel JC, Shao Y, Bassler BL. 2011. AphA and LuxR/HapR
572 reciprocally control quorum sensing in vibrios. Genes Dev 25:397-408.
573 35. Shao Y, Feng L, Rutherford S, Papenfort K, Bassler B. 2013. Functional
574 determinants of the quorum-sensing non-coding RNAs and their roles in target
575 regulation. EMBO J 32:2158-71.
576 36. Hunter GA, Keener JP. 2014. Mechanisms underlying the additive and
577 redundant Qrr phenotypes in Vibrio harveyi and Vibrio cholerae. J Theor Biol
578 340:38-49.
579 37. Lenz DH, Mok KC, Lilley BN, Kulkarni RV, Wingreen NS, Bassler BL. 2004. The
580 small RNA chaperone Hfq and multiple small RNAs control quorum sensing in
581 Vibrio harveyi and Vibrio cholerae. Cell 118:69-82.

582 38. Joseph S, Colwell R, Kaper J. 1982. Vibrio parahaemolyticus and related
583 halophilic Vibrios. Crit Rev Microbiol 10:77-124.
584 39. Colwell R, Kaper J, Joseph S. 1977. Vibrio cholerae, Vibrio parahaemolyticus, and
585 other vibrios: occurrence and distribution in Chesapeake Bay. Science (New
586 York, NY) 198:394-6.
587 40. Thompson F, Iida T, Swings J. 2004. Biodiversity of vibrios. Microbiology and
588 molecular biology reviews : MMBR 68:403-31.
589 41. Nair GB, Ramamurthy T, Bhattacharya SK, Dutta B, Takeda Y, Sack DA. 2007.
590 Global dissemination of Vibrio parahaemolyticus serotype O3:K6 and its
591 serovariants. Clin Microbiol Rev 20:39-48.
592 42. O'Boyle N, Boyd A. 2014. Manipulation of intestinal epithelial cell function by
593 the cell contact-dependent type III secretion systems of Vibrio parahaemolyticus.
594 Front Cell Infect Microbiol 3.
595 43. Allison C, Hughes C. 1991. Bacterial swarming: an example of prokaryotic
596 differentiation and multicellular behaviour. Sci Prog 75:403-22.
597 44. McCarter LL. 1998. OpaR, a Homolog of Vibrio harveyi LuxR, Controls Opacity
598 of Vibrio parahaemolyticus, p 3166-73, J Bacteriol, vol 180.
599 45. ZT G, LL M. 2003. Multiple regulators control capsular polysaccharide
600 production in Vibrio parahaemolyticus. J Bacteriol 185:5431-41.

601 46. Gode-Potratz CJ, McCarter LL. 2011. Quorum sensing and silencing in Vibrio
602 parahaemolyticus. J Bacteriol 193:4224-37.
603 47. Jaques S, McCarter L. 2006. Three new regulators of swarming in Vibrio
604 parahaemolyticus. J Bacteriol 188:2625-35.
605 48. Gregory GJ, Morreale DP, Carpenter MR, Kalburge SS, Boyd EF. 2019. Quorum
606 Sensing Regulators AphA and OpaR Control Expression of the Operon
607 Responsible for Biosynthesis of the Compatible Solute Ectoine. Appl Environ
608 Microbiol 85:1543-19.
609 49. Gregory GJ, Morreale DP, Boyd EF. 2020. CosR Is a Global Regulator of the
610 Osmotic Stress Response with Widespread Distribution among Bacteria. Appl
611 Environ Microbiol 86:120-20.
612 50. Whitaker WB, Richards GP, Boyd EF. 2014. Loss of sigma factor RpoN increases
613 intestinal colonization of Vibrio parahaemolyticus in an adult mouse model.
614 Infect Immun 82:544-56.
615 51. Eickhoff M, Fei C, Huang X, Bassler B. 2021. LuxT controls specific quorum-
616 sensing-regulated behaviors in Vibrionaceae spp. via repression of qrr1,
617 encoding a small regulatory RNA. PLoS Genet 17:e1009336.
618 52. Schaefer J, Engl C, Zhang N, Lawton E, Buck M. 2015. Genome wide interactions
619 of wild-type and activator bypass forms of σ54. Nucleic Acids Res 43:7280-91.

620 53. Zafar MA, Carabetta VJ, Mandel MJ, Silhavy TJ. 2014. Transcriptional occlusion
621 caused by overlapping promoters. Proc Natl Acad Sci U S A 111:1557-61.
622 54. Reichenbach B, Göpel Y, Görke B. 2009. Dual control by perfectly overlapping
623 sigma 54- and sigma 70- promoters adjusts small RNA GlmY expression to
624 different environmental signals. Mol Microbiol 74:1054-70.
625 55. Keane OM, Dorman CJ. 2003. The gyr genes of Salmonella enterica serovar
626 Typhimurium are repressed by the factor for inversion stimulation, Fis. Mol
627 Genet Genomics 270:56-65.
628 56. Browning DF, Grainger DC, Beatty CM, Wolfe AJ, Cole JA, Busby SJ. 2005.
629 Integration of three signals at the Escherichia coli nrf promoter: a role for Fis
630 protein in catabolite repression. Mol Microbiol 57:496-510.
631 57. Kelly A, Goldberg MD, Carroll RK, Danino V, Hinton JCD, Dorman CJ. 2004. A
632 global role for Fis in the transcriptional control of metabolism and type III
633 secretion in Salmonella enterica serovar Typhimurium. Microbiology 150:2037-
634 2053.
635 58. Grainger DC, Hurd D, Goldberg MD, Busby SJ. 2006. Association of nucleoid
636 proteins with coding and non-coding segments of the Escherichia coli genome.
637 Nucleic Acids Res 34:4642-52.

638 59. Wang Q, Liu Q, Ma Y, Rui H, Zhang Y. 2007. LuxO controls extracellular
639 protease, haemolytic activities and siderophore production in fish pathogen
640 Vibrio alginolyticus. J Appl Microbiol 103:1525-34.
641 60. Livak KJ, Schmittgen TD. 2001. Analysis of relative gene expression data using
642 real-time quantitative PCR and the 2(-Delta Delta C(T)) Method. Methods 25:402-
643 8.
644 61. Karunakaran R, Mauchline TH, Hosie AH, Poole PS. 2005. A family of promoter
645 probe vectors incorporating autofluorescent and chromogenic reporter proteins
646 for studying gene expression in Gram-negative bacteria. Microbiology 151:3249-
647 56.
648 62. Gibson DG. 2011. Enzymatic assembly of overlapping DNA fragments. Methods
649 Enzymol 498:349-61.
650 63. Chaparian RR, Tran MLN, Conrad LCM, Rusch DB, Kessel JCv. 2019. Global H-
651 NS counter-silencing by LuxR activates quorum sensing gene expression.
652 64. Chaparian RR, Olney SG, Hustmyer CM, Rowe-Magnus DA, van Kessel JC. 2016.
653 Integration host factor and LuxR synergistically bind DNA to coactivate quorum-
654 sensing genes in Vibrio harveyi. Mol Microbiol 101:823-40.
655 65. Jutras BL, Verma A, Stevenson B. 2012. Identification of novel DNA-binding
656 proteins using DNA-affinity chromatography/pull down. Curr Protoc Microbiol
657 Chapter 1:Unit1F.1.

658 66. Jutras BL, Liu Z, Brissette CA. 2010. Simultaneous isolation of Ixodidae and
659 bacterial (Borrelia spp.) genomic DNA. Curr Protoc Microbiol C 1:E.2.
660 67. Whitaker WB, Parent MA, Naughton LM, Richards GP, Blumerman SL, Boyd EF.
661 2010. Modulation of Responses of Vibrio parahaemolyticus O3:K6 to pH and
662 Temperature Stresses by Growth at Different Salt Concentrations. Appl Environ
663 Microbiol 76:4720-9.
664 68. Makino K, Oshima K, Kurokawa K, Yokoyama K, Uda T, Tagomori K, Iijima Y,
665 Najima M, Nakano M, Yamashita A, Kubota Y, Kimura S, Yasunaga T, Honda T,
666 Shinagawa H, Hattori M, Iida T. 2003. Genome sequence of Vibrio
667 parahaemolyticus: a pathogenic mechanism distinct from that of V cholerae.
668 Lancet 361:743-9.
669 69. Dehio C, Meyer M. 1997. Maintenance of broad-host-range incompatibility group
670 P and group Q plasmids and transposition of Tn5 in Bartonella henselae
671 following conjugal plasmid transfer from Escherichia coli. J Bacteriol 179:538-40.
672 70. Philippe N, Alcaraz JP, Coursange E, Geiselmann J, Schneider D. 2004.
673 Improvement of pCVD442, a suicide plasmid for gene allele exchange in bacteria.
674 Plasmid 51:246-55.
675 71. Guzman LM, Belin D, Carson MJ, Beckwith J. 1995. Tight regulation, modulation,
676 and high-level expression by vectors containing the arabinose PBAD promoter. J
677 Bacteriol 177:4121-30.

678

679 **Table 1**. Strains and plasmids used in this study

Strain or plasmid	Genotype	Source
Vibrio parahaemolyticus		
RIMD2210633	O3:K6 clinical isolate; StrR	(67, 68)
SSK2099 (Δ*luxO*)	RIMD2210633 Δ*luxO*; StrR	(14)
SSK2516 (Δ*opaR*)	RIMD2210633 Δ*opaR*; StrR	(14)
WBW2670(Δ*rpoN)*	RIMD2210633 Δ*rpoN*; StrR	(50)
JGT2019 (Δ*rpoN*/Δ*luxO)*	RIMD2210633 Δ*rpoN*/Δ*luxO*; StrR	This study
JGT2020 (Δ*rpoN*/Δ*qrr2*)	RIMD2210633 Δ*rpoN*/Δ*qrr2*; StrR	This study
JGT2021 (Δ*rpoN*/Δ*fis*)	RIMD2210633 Δ*rpoN*/Δ*fis*; StrR	This study
JGTqrr1345 (Δ*qrr2*)	RIMD2210633 Δ*qrr2*; StrR	This study
GJGqrr-null	RIMD2210633 Δ*qrr*3,2,1,4,5; StrR	This study
JGTqrr1	RIMD2210633 Δ*qrr3,2,4,5*; StrR	This study
JGTqrr2	RIMD2210633 Δ*qrr3,1,4,5*; StrR	This study
JGTqrr3	RIMD2210633 Δ*qrr2,1,4,5*; StrR	This study
JGTqrr4	RIMD2210633 Δ*qrr3,2,1,5*; StrR	This study
JGTqrr5	RIMD2210633 Δ*qrr3,2,1,4*; StrR	This study
RIMD2210633 p*opaR*	RIMD2210633 harboring pBAD*opaR*	This study
RIMD2210633 pEV	RIMD2210633 harboring pBAD33	This study
Δ*opaR* p*opaR*	Δ*opaR* harboring pBAD*opaR*	This study
Δ*opaR* pEV	Δ*opaR* harboring pBAD33	This study
Δ*rpoN* p*opaR*	Δ*rpoN* harboring pBAD*opaR*	This study
Δ*rpoN* pEV	Δ*rpoN* harboring pBAD33	This study
Δ*rpoN* p*qrr2*-10CCC	Δ*rpoN* harboring pRUP*qrr2* with mutated -10 promoter	This study
Escherichia coli		
Dh5α	Δ*lac pir*	Thermo Fisher Scientific
B2155*λpir*	Δ*dapA::erm pir*; for conjugations	(69)
Plasmids		
pDS132	Suicide vector; CmR; *sacB* (sucrose intolerant)	(70)
pBAD33	Expression vector; *araB* promoter; Cm^r	(71)

pBAD*opaR*	pBAD33 with *opaR*, CmR	This study
pRU1064	promoterless-gfpUV, AmpR, TetR, IncP origin	(61)
pRUP*qrr2*	pRU1064 with P*qrr2-gfp*, AmpR, TetR	This study
pRUP*qrr*2-10CCC	pRUP*qrr2* with mutated -10 to CCC promoter, AmpR, TetR	This study
pRUP*opaR*	pRU1064 with P*opaR-gfp*, AmpR, TetR	This study

680

681

682 **Table 2**. Primers used in this study

Primer	Sequence (5′-3′)	Length (bp)
Mutant		
SOEqrr1A	catgcgatatcgagctGAATTGCGTTGTTGACCG	554
SOEqrr1B	aaagctgatGGGTCGCTAATATATCAGCATG	
SOEqrr1C	agcgacccatccATCAGCTTTTCGTGTTAACTAG	543
SOEqrr1D	attcccgggagagctGATATGCCGGAAGTCTCG	
SOEqrr1FLFwd	TTCATCGAGGAACAACGTGC	1873
SOEqrr1FLRev	GCCGGGCAATTATGAGCTAG	
SOEqrr2A	*TCTAGA*AGAGACGGGTTAATACGACGA	456
SOEqrr2B	TCAAAGCTTTATTTTTGGGCA	
SOEqrr2C	TGAACAACGTTACTTACGTGCTTTGC	461
SOEqrr2D	*GAGCTC*ACCGCGCTCAACAACTAATG	
SOEqrr2FLFwd	TTGATGGCGCTACGATTGGT	1237
SOEqrr2FLRev	CGCTAAGGTTGCAATGCTCG	
SOEqrr3A	*CACTCTAGA*ATTGCTCAAGTGGTGGCTTT	560
SOEqrr3B	TTTATATGCCCGAAAATCGTG	
SOEqrr3C	cacgattttcgggcatataaaCGGCTACTGCTCTCCTTTAT	607
SOEqrr3D	cacgagctcGTGTTGGGAACTGGTCCAAG	
SOEqrr3FLFwd	GCAAAATGACACTGCCAGAA	1887
SOEqrr3FLRev	GTTGCTTTATGCACCGGAAT	
SOEqrr4A	catgcgatatcgagctGCGCAAGGTTGTCGTAG	477
SOEqrr4B	gtctctagaaGATGCGTGCCAACTTTAAAAAAG	
SOEqrr4C	ggcacgcatcttCTAGAGACCGATAATATTCACATT	517
SOEqrr4D	attcccgggagagctATTACCTTGGGGCAACATGC	
SOEqrr4FLFwd	CGGCTTTGAGTCTGTGCAAT	1796
SOEqrr4FLRev	GCGACTACCCTACCCGTTTA	
SOEqrr5A	catgcgatatcgagctTTCAAGTTATGAATAGCGATG	523
SOEqrr5B	cctgaagatGCTGTAGGAACTTATTAG	
SOEqrr5C	tacagcgcATCTTCAGGTTTCCTATCTCTA	525
SOEqrr5D	attcccgggagagctTTTCTTGGCTTCAACACG	
SOEqrr5FLFwd	TCTTTGGGGAGCTGTTCGAT	1853
SOEqrr5FLRev	GGCGTTTACTGGTCTGCATC	
Pqrr2SDM10B	cttaagaagggtcgagaag**GGG**tatgcattaatcatgccaattttca	
Pqrr2SDM10C	catgattaatgcatac**CCC**ttctcgacccttcttaagccgagggtcacctag	

Expression		
pBADopaR_fwd	*TACTCTAGA*ACAACAACTCAAATGGCAAGGAAA	670
pBADopaR_rev	*CTAAAGCTT*TGAGCTTTAGTGTTCGCGATTG	
qPCR		
opaR_fwd	CCATGTTGTCCGTCAGTTCTCG	158
opaR_rev	GAGTTGATGCGCTCCACTCG	
aphA_fwd	AGCCACCAACAAGTTTACCG	140
aphA_rev	CATTCTCCAAGAGCGCTACG	
qrr1_fwd	CTCGGGTCACCTAGCCAACT	85
qrr1_rev	AAGAAGCCAATAGGCAGTCG	
qrr2_fwd	CTTAAGCCGAGGGTCACCTA	95
qrr2_rev	ATAGCCAACCGCAATAATCG	
qrr3_fwd	CTTAAGCCGAGGGTCACCTA	95
qrr3_rev	ATAGCCAACCGCAAAGAGTG	
qrr4_fwd	ACCCTTATTAAGCCGAGGGTCA	101
qrr4_rev	AACGCCAATCACAAGAAAGG	
qrr5_fwd	TCTAAGCCGAGGGTCACCTA	95
qrr5_rev	AAAAGCCAACCACAAGGTGT	
16S_fwd	ACCGCCTGGGGAGTACGGTC	234
16S_rev	TTGCGCTCGTTGCGGGACTT	
GFP reporter		
pRUPopaR_fwd	tagatagagagagagagagaACTGTGCTCAATTTAGTTTG	358
pRUPopaR_rev	actcatttttttcttcctccaATCCATTTTCCTTGCCATTTG	
pRUPqrr2_fwd	actcatttttttcttcctccaAGAAGTATTATGCATTAATCATGC	377
pRUPqrr2_rev	tagatagagagagagagagaTTCTTTAGTGCTAAGTCATG	
EMSA		
Pqrr2_fwd	GAAGGGTCGAGAAGTATTATGC	290
Pqrr2_rev	AAGTATGAAATAGTGTCGTAGTTAATATT	
Pqrr2_1A_fwd	GAAGGGTCGAGAAGTATTATG	120
Pqrr2_1A_rev	AATTAAGTTTTGTTTTTTGCAAAAATTTAT	
Pqrr2_1B_fwd	GATATTGCCTATATAAATTTTTGCAAAAA	119
Pqrr2_1B_rev	ATTTTATTTTCATTTACATTTTGACTAAC	
Pqrr2_1C_fwd	GTAAATGAAAATAAAATGTTAACGAGTTG	110
Pqrr2_1C_rev	AAGTATGAAATAGTGTCGTAGTTAATATT	
Mutagenesis		
Pqrr2SDM10_GA fwd	tagatagagagagagagagaTTCTTTAGTGCTAAGTCATG	377
Pqrr2SDM10_GA	actcatttttttcttcctccaAGAAG**GGG**TATGCATTAATC	

rev		
SOEqrr2A	*TCTAGA*AGAGACGGGTTAATACGACGA	500
SOEqrr2SDM_B	CATGATTAATGCATA**CCC**CTTCTCGACCCTTCTTA AGCCGAGGGTCACCTAG	
SOEqrr2SDM_C	CTTAAGAAGGGTCGAGAAG**GGG**TATGCATTAATC ATGCCAATTTTCA	605
SOEqrr2D	*GAGCTC*ACCGCGCTCAACAACTAATG	

683

684

685 **Figure legends**

686

687 **Figure 1**: *Vibrio parahaemolyticus* quorum sensing pathway. Autoinducers (AIs) are
688 synthesizes internally by three synthases and then excreted outside the cell. At low cell
689 density, three histidine-kinase receptors are free of AIs, therefore act as kinases,
690 phosphorylating LuxU and ultimately LuxO. LuxO-P activates RpoN and, along with
691 Fis positively regulates transcription of five small quorum regulatory RNAs (Qrr
692 sRNAs). The Qrr sRNAs, along with Hfq, stabilize *aphA* transcripts and destabilize *opaR*
693 transcripts. In addition, AphA is a negative regulator of *opaR* expression. At high cell
694 density, LuxO is unphosphorylated and inactivate, no *qrrs* are transcribed, *opaR* is
695 expressed and *aphA* is repressed. OpaR positively regulates capsule polysaccharide
696 production (CPS), biofilm formation, type 6 secretion system-1, and the type IV pilin
697 MSHA, among other genes. OpaR negatively regulates swarming motility, surface
698 sensing and two contact dependent secretion systems T3SS-1 and T6SS-1.

699 **Figure 2: A.** Wild type (WT) and QS mutant strains production of capsule
700 polysaccharide (CPS) and colony morphology on Congo red plates. **B**. Biofilm assay
701 from cultures grown for 24 h, stagnant and stained with crystal violet. Images are
702 representatives from three bio-reps. Biofilm quantification of three bio-reps in duplicate.
703 Statistics calculated using a Student's t-test. ***, P-value <0.001

Figure 3: Quantitative real time PCR expression analysis of cells grown to 0.1 (**A, C)** or 0.5 OD (**B, D)** in LB media supplemented with 3% NaCl. Expression of *opaR* and *aphA* relative to WT RIMD2210633 and normalized to 16S housekeeping gene. Means and standard error of at least two biological replicates shown. Statistics calculated using a Student's t-test. *, P-value <0.05; **, P-value <0.01.

Figure 4: Quantitative real time PCR expression analysis of cells grown to 0.1 (**A, C**) or 0.5 OD (**B, D**) in LB media supplemented with 3% NaCl. Expression of *qrr1-5* relative to wild type RIMD2210633 and normalized to 16S housekeeping gene. Expression of *qrr4* not detected in mutant strains. Means and standard error of at least two biological replicates shown. Statistics calculated using a Student's t-test. *, P-value <0.05; **, P-value <0.01; ***, P-value <0.001.

Figure 5: A. P*qrr2*-gfp reporter assay of *qrr2* in *luxO* and *rpoN* mutants. **B**. P*opaR*-gfp reporter assays in a single qrr2 deletion mutant and a quadruple mutant with only *qrr2* present. Cultures grown for 20 h in LB 3% NaCl. Means and standard error of at least three biological replicates shown. Statistics calculated using a one-way ANOVA and Tukey-Kramer *post-hoc* test. **, P-value <0.01

Figure 6: A. Analysis of *qrr2* regulatory region indicates overlapping sigma-54 and sigma-70 promoters. **B.** P*qrr2* GFP reporter assay of *qrr2* in Δ*rpoN* relative to wild type and mutated putative -10 RpoD binding site are indicated by asterisks. Means and

723 standard error of three biological replicates shown. Statistics calculated using a one-way
724 ANOVA and Tukey-Kramer *post-hoc* test. ***, P-value <0.001

725 **Figure 7: A.** Regulatory region of *qrr2* depicted. Lines represent EMSA probes and blue
726 triangles represent putative Fis binding sites using Virtual Footprint prediction
727 software. Numbers indicate Fis binding site distance from *qrr2* transcriptional start site.
728 **B.** Electrophoretic mobility shift assays of P*qrr2* with purified Fis protein using four *qrr2*
729 regulatory region DNA probes **C.** pRUP*qrr2* reporter assays in Δ*rpoN* and Δ*rpoN*/Δ*fis*
730 deletion mutants mutants relative to WT. Cultures grown for 20 h in LB 3% NaCl.
731 Means and standard error of at least three biological replicates shown. Statistics
732 calculated using a one-way ANOVA and Tukey-Kramer *post-hoc* test. ***, P-value
733 <0.001.

734 **Figure 8:** Model for *qrr2* transcription in the Δ*luxO* and Δ*rpoN* mutants. In the Δ*luxO*
735 mutant, under certain conditions RpoN will be bound to the *qrr2* RpoN -24 -12
736 promoter region. RpoN bound at the promoter will be aided by Fis. This will prevent
737 sigma-70 from binding. In the absence of RpoN (sigma-54), RpoD (sigma-70) can bind to
738 the -35 -10 promoter region to initiate transcription. In the absence of Fis in the rpoN
739 mutant transcription by RpoD is increased further as in the Δ*rpoN*/Δ*fis* mutant.

740

741 **Supplementary Figure Legends**

742 **Figure S1:** Complementation analysis of Δ*rpoN* mutant with *opaR.* Expression vectors
743 pBAD*opaR* and pBAD33 (empty vector) were conjugated into the *V. parahaemolyticus*
744 *rpoN* mutant and spot inoculated on to congo red plates supplemented with 0.1%
745 arabinose and 5 μg/ml chloramphenicol.
746 **Figure S2:** Gene expression analysis of cells grown to 0.1 OD and 0.5 OD in LB 3%
747 NaCl. Expression of *qrr1* to *qrr5* at 0.1 OD relative to 0.5 OD, and normalized to 16S
748 housekeeping gene. Means and standard error of at least two biological replicates
749 shown. Expression of *qrr4* not detected at 0.5 OD. Statistics calculated using a Student's
750 t-test. *, P-value <0.05; **, P-value <0.01.
751 **Figure S3: A.** Quantitative real time PCR (qPCR) analysis of *opaR* and **B.** *aphA*. A. qPCR
752 analysis in single D*rpoN* mutant and double D*rpoN*/D*qrr2* mutant. Two bio-reps in
753 duplicate performed. Means and standard error of at least two biological replicates
754 shown. Statistics calculated using a Student's t-test. **, P-value <0.01
755 **Figure S4:** Phenotypic analysis of Δ*rpoN*/Δ*qrr2* double deletion mutant
756 **A.** CPS production in double mutant. **B.** Biofilm assay and quantification from cultures
757 grown for 24 h stagnant and stained with crystal violet. Three bio-reps in duplicate
758 performed. Statistics calculated using a one-way ANOVA and Tukey-Kramer *post-hoc*
759 test. ***, P-value <0.001
760 **Figure S5.** The *V. parahaemolyticus* Qrr sRNAs regulatory and coding regions were
761 aligned using T-COFFEE Multiple Sequence Aligner. The RpoN conserved binding site

762 at -24 -12 and the transcriptional start site are labeled. The red lines indicate the RpoN
763 promoter region with a highly conserved TGGC(-24) and TGC(-12). An asterisk
764 indicates conserved nucleotides among all five *qrrs*. The blue box depicts the putative
765 RpoD promoter of *qrr2*.

766 **Figure S6.** The *qrr2* gene sequence alignment from *V. harveyi* ATCC 33843, *V. campbellii*
767 ATCC BAA-1116, *V. parahaemolyticus* RIMD2210633 *and V. alginolyticus*
768 FDAARGOS_114 and the regulatory regions aligned using CLUSTALW. The sigma-54
769 conserved -24 -12 promoter binding sites are shown in blue boxes and the sigma-70 -35
770 and -10 promoter are shown in red boxes. The conserved nucleotides among the *qrr2*
771 genes are shown by an asterisk. The data shows that the -10 promoter site is conserved
772 between *V. parahaemolyticus* and *V. alginolyticus* with a 1-bp polymorphism in *V. harveyi*.
773 Similarly, the -35 site is highly conserved between *V. parahaemolyticus* and *V.*
774 *alginolyticus* but contains several polymorphisms in *V. harveyi*.

775 **Figure S7.** Phylogenetic tree of the *qrr* genes in *V. harveyi* ATCC 33843, *V. campbellii*
776 ATCC BAA-1116, *V. parahaemolyticus* RIMD2210633 *and V. alginolyticus*
777 FDAARGOS_114. The evolutionary history was inferred by using the Maximum
778 Likelihood method and Jukes-Cantor model in MEGA X (1,2). The tree with the highest
779 log likelihood (-467.92) is shown. The percentage of trees in which the associated taxa
780 clustered together is shown next to the branches. Initial tree(s) for the heuristic search
781 were obtained automatically by applying Neighbor-Join and BioNJ algorithms to a

782 matrix of pairwise distances estimated using the Maximum Composite Likelihood
783 (MCL) approach, and then selecting the topology with superior log likelihood value. A
784 discrete Gamma distribution was used to model evolutionary rate differences among
785 sites (3 categories (+*G*, parameter = 0.2492)). The tree is drawn to scale, with branch
786 lengths measured in the number of substitutions per site. This analysis involved 20
787 nucleotide sequences.

788 1. Jukes T.H. and Cantor C.R. (**1969**). Evolution of protein molecules. In Munro HN,
789 editor, *Mammalian Protein Metabolism*, pp. 21-132, Academic Press, New York.
790 2. Kumar S., Stecher G., Li M., Knyaz C., and Tamura K. (**2018**). MEGA X: Molecular
791 Evolutionary Genetics Analysis across computing platforms. *Molecular Biology and*
792 *Evolution* **35**:1547-1549.
793 3. Felsenstein J. (**1985**). Confidence limits on phylogenies: An approach using the
794 bootstrap. *Evolution* **39**:783-791.

795 **Figure S8:** Phenotypes of *qrr* deletion mutants. **A.** Swarming assay conducted on heart-
796 infusion media incubated at 30˚C for 48 h. **B.** Swimming motility assay conduced on
797 semi-solid agar plates grown at 37˚C for 24 h. Swimming plate quantification of three
798 biological replicates. Statistics calculated using Student's t-test relative to Wild-type. ***,
799 P-value <0.001. **C.** CPS assays conducted of strains of interest. Colonies grown on
800 Congo red plates for 48 h at 30˚C prior to imaging.

Figure S9. Phenotype of qrr2 single deletion mutant. **A.** CPS production Strains of interest were inoculated on congo red plates and incubated for 48 hours at 30°C. Wild Type RIMD2210633 was used as a positive control and Δ*opaR* was used as a negative control. **B**. Swarming motility. Strains of interest were inoculated on swarming plates and incubated for 48 hours at 30°C.

Figure S10: DNA affinity pull-down of *qrr2* regulatory region (+) used to identify candidate regulators. Increasing concentrations of NaCl used to elute bound proteins. VP1624 coding region used as negative control bait DNA (-). Adjacent elutions used for comparison purposes. Boxes indicate chosen bands sent for Mass Spectrometry analysis. Boxes labeled N chosen to eliminate cross-over.

Figure S11: List of candidates identified in DNA affinity pull-down. Candidates divided into three categories, based on previously determined function. Fis is highlighted in red, as the target candidate in this study.

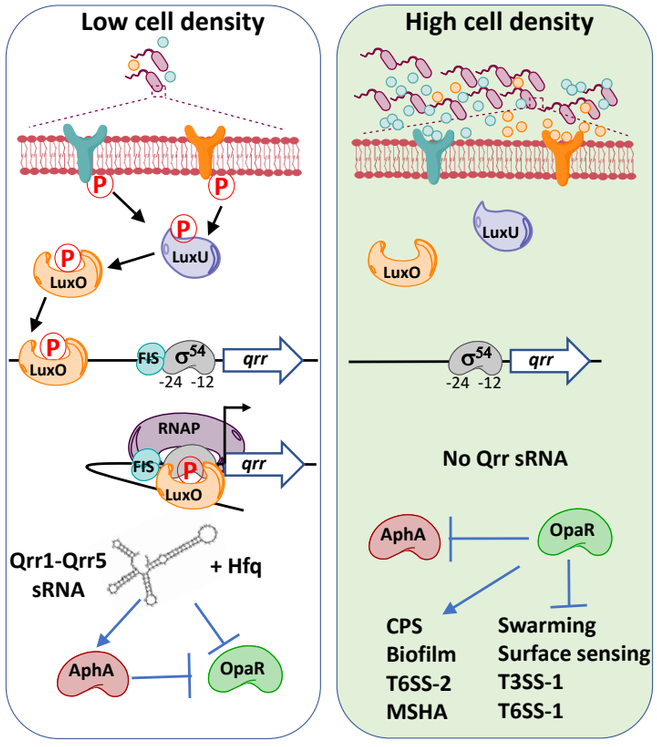

Figure 1. *Vibrio parahaemolyticus* quorum sensing pathway. Autoinducers (AIs) are synthesizes internally by three synthases and then excreted outside the cell. At low cell density, three histidine-kinase receptors are free of AIs, therefore act as kinases, phosphorylating LuxU and ultimately LuxO. LuxO-P activates RpoN and, along with Fis positively regulates transcription of five small quorum regulatory RNAs (Qrr sRNAs). The Qrr sRNAs, along with Hfq, stabilize *aphA* transcripts and destabilize *opaR* transcripts. In addition, AphA is a negative regulator of *opaR* expression. At high cell density, LuxO is unphosphorylated and inactivate, no *qrrs* are transcribed, *opaR* is expressed and *aphA* is repressed. OpaR positively regulates capsule polysaccharide production (CPS), biofilm formation, type 6 secretion system-1, and the type IV pilin MSHA, among other genes. OpaR negatively regulates swarming motility, surface sensing and two contact dependent secretion systems T3SS-1 and T6SS-1.

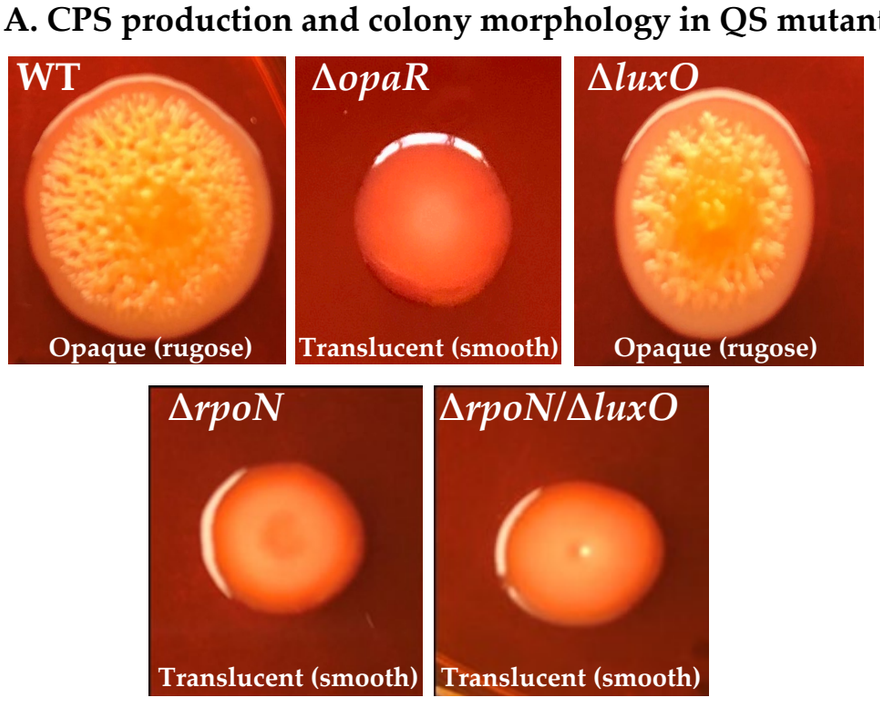

Figure 2: A. Wild type (WT) and QS mutant strains production of capsule polysaccharide (CPS) and colony morphology on Congo red plates. **B**. Biofilm assay from cultures grown for 24 hrs, stagnant and stained with crystal violet. Images are representatives from three bio-reps. Biofilm quantification of three bio-reps in duplicate. Statistics calculated using a Student's t-test. ***, P-value <0.001

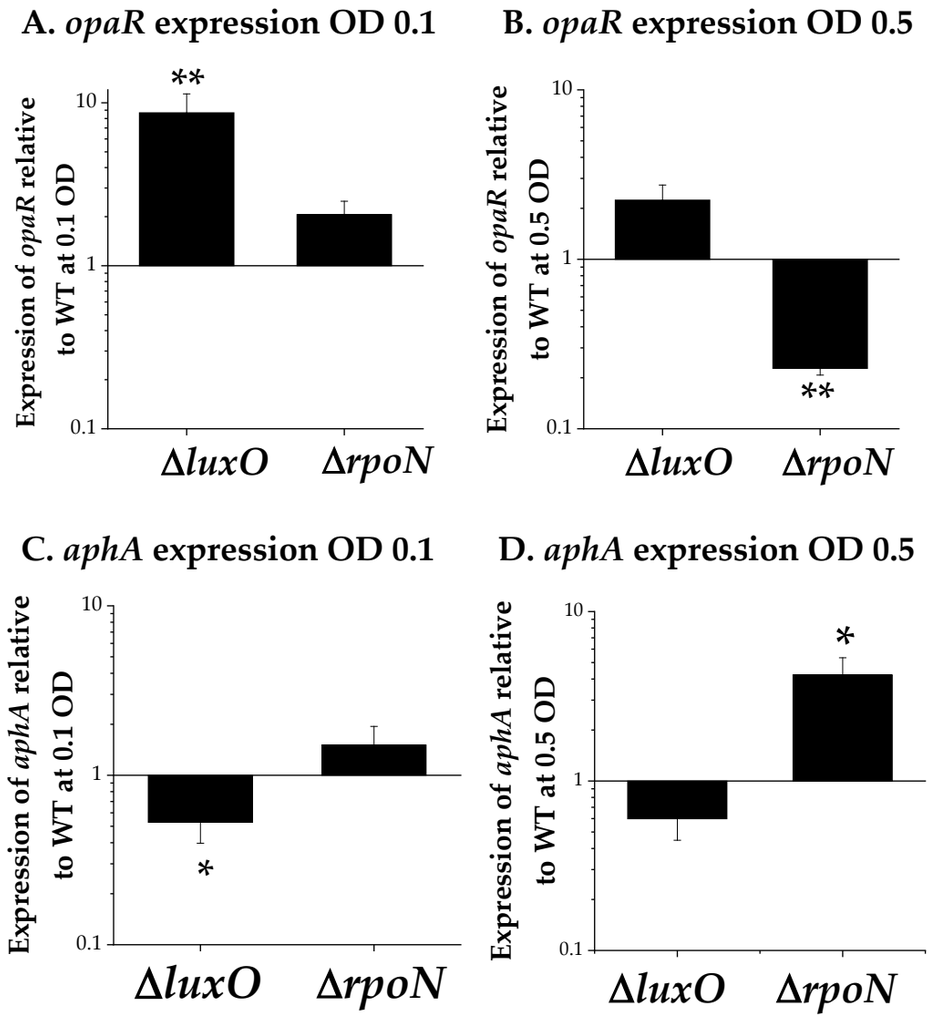

Figure 3: Quantitative real time PCR expression analysis of cells grown to 0.1 (**A, C)** or 0.5 OD (**B, D)** in LB media supplemented with 3% NaCl. Expression of *opaR* and *aphA* relative to WT RIMD2210633 and normalized to 16S housekeeping gene. Means and standard error of at least two biological replicates shown. Statistics calculated using a Student's t-test. *, P-value <0.05; **, P-value <0.01.

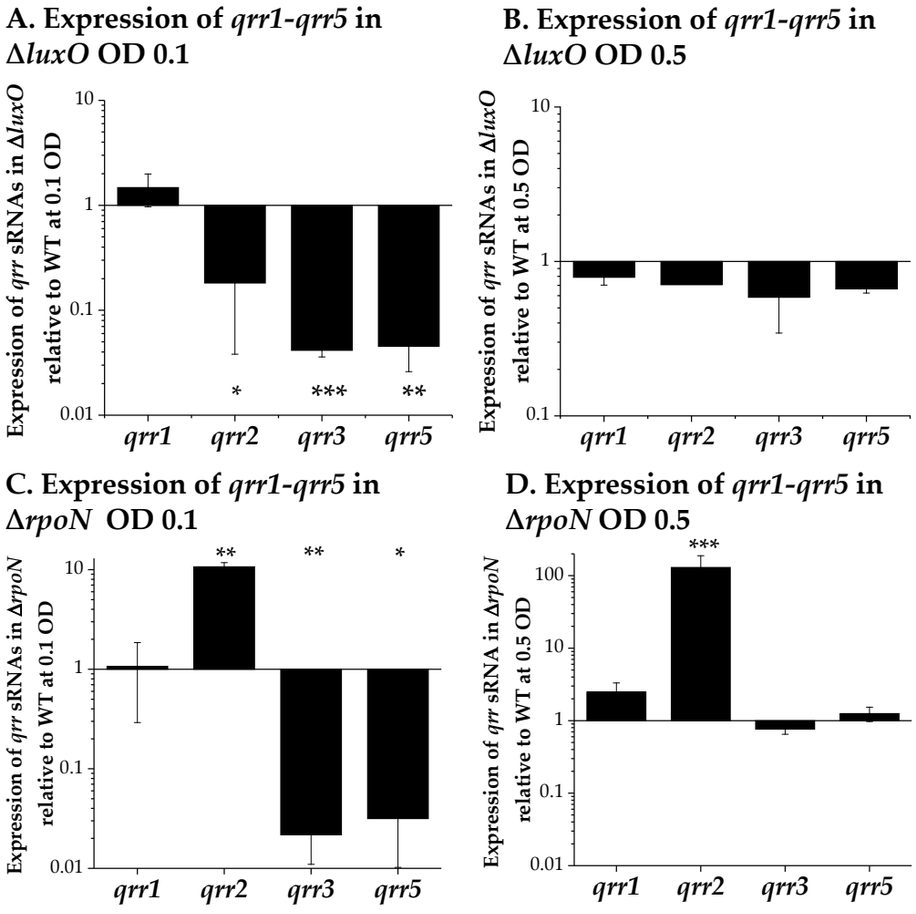

Figure 4: Quantitative real time PCR expression analysis of cells grown to 0.1 (**A, C**) or 0.5 OD (**B, D**) in LB media supplemented with 3% NaCl. Expression of *qrr1-5* relative to wild type RIMD2210633 and normalized to 16S housekeeping gene. Expression of *qrr4* not detected in mutant strains. Means and standard error of at least two biological replicates shown. Statistics calculated using a Student's t-test. *, P-value <0.05; **, P-value <0.01; ***, P-value <0.001.

A. P*qrr2-gfp* expression in Δ*luxO* and Δ*rpoN* mutants

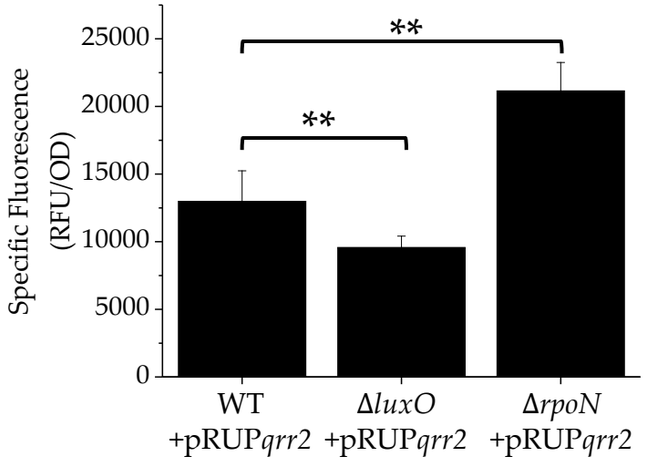

B. P*opaR-gfp* expression in Δ*qrr2* mutant and quadruple Δ*qrr1,3,4,5* mutant

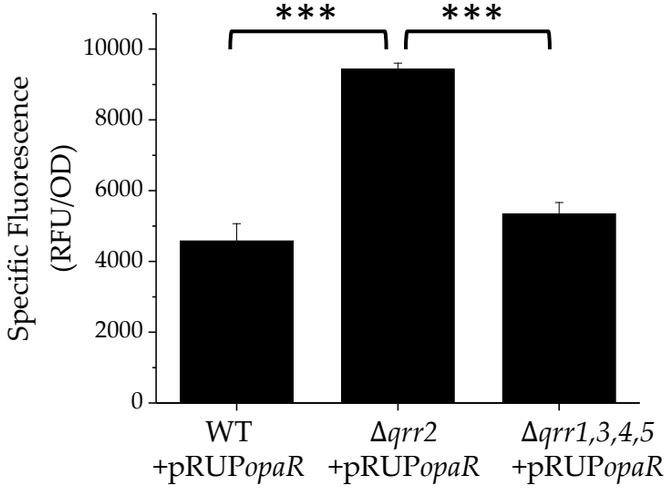

Figure 5: A. P*qrr2*-gfp reporter assay of *qrr2* in *luxO* and *rpoN* mutants. **B**. P*opaR*-gfp reporter assays in a single qrr2 deletion mutant and a quadruple mutant with only *qrr2* present. Cultures grown for 20 hrs in LB 3% NaCl. Means and standard error of at least three biological replicates shown. Statistics calculated using a one-way ANOVA and Tukey-Kramer *post-hoc* test. **, P-value <0.01

A. Putative sigma-70 -10 -35 promoter present in *qrr2* regulatory region

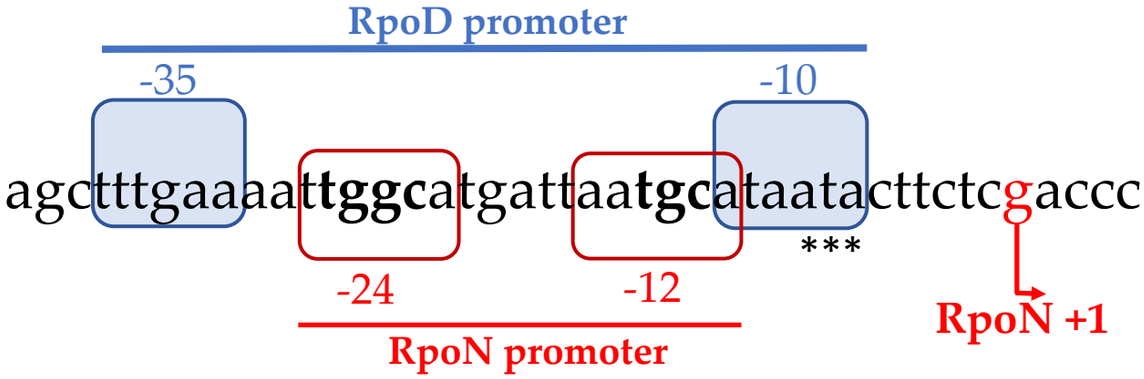

B. Mutation of putative sigma-70 -10 promoter site and expression of *qrr2*

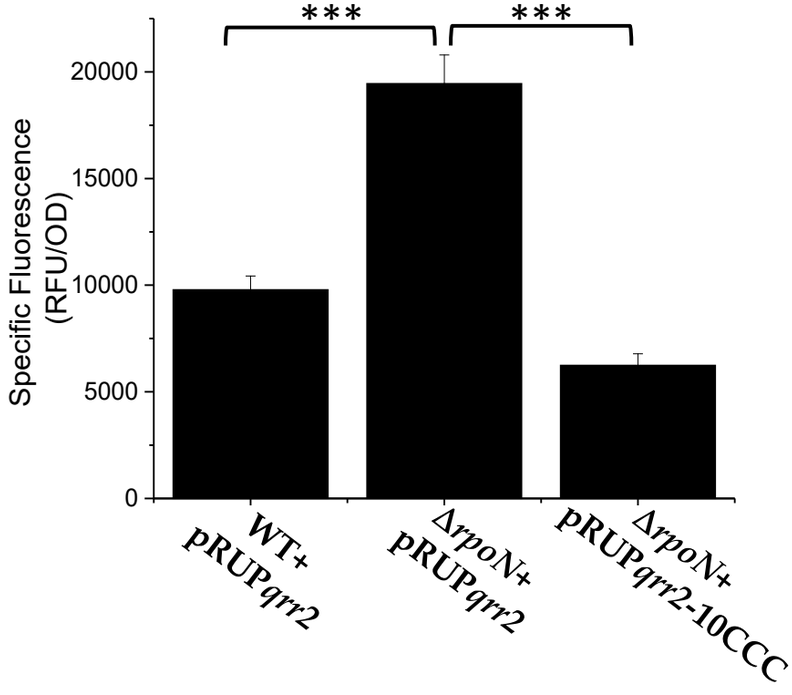

Figure 6: A. Analysis of *qrr2* regulatory region indicates overlapping sigma-54 and sigma-70 promoters. **B.** P*qrr2* GFP reporter assay of *qrr2* in Δ*rpoN* relative to wild type and mutated putative -10 RpoD binding site are indicated by asterisks. Means and standard error of three biological replicates shown. Statistics calculated using a one-way ANOVA and Tukey-Kramer *post-hoc* test. ***, P-value <0.001

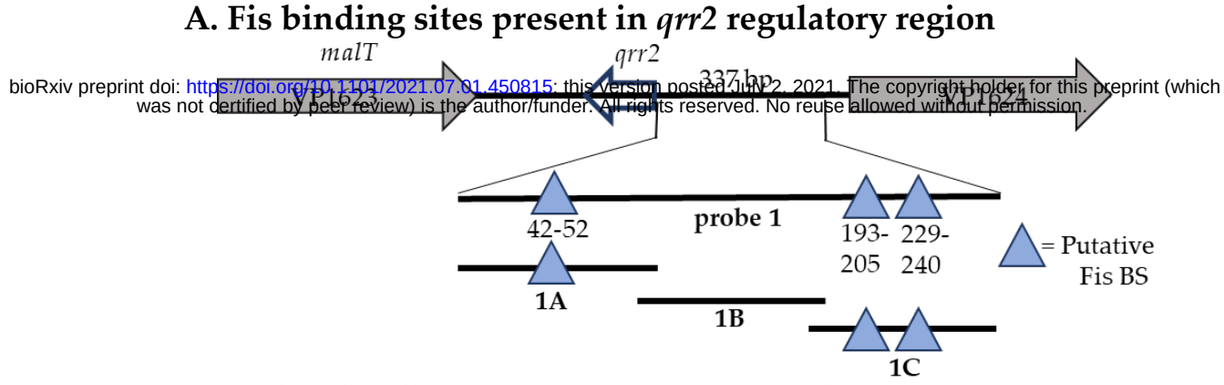

Figure 7: A. Regulatory region of *qrr2*. Lines represent EMSA probes and blue triangles represent putative Fis binding sites using Virtual Footprint prediction software. Numbers indicate Fis binding site distance from *qrr2* transcriptional start site. **B.** Electrophoretic mobility shift assays of P*qrr2* with purified Fis protein using four *qrr2* regulatory region DNA probes **C.** pRUP*qrr2* reporter assays in Δ*rpoN* and Δ*rpoN*/Δ*fis* deletion mutants mutants relative to WT. Cultures grown for 20 hrs in LB 3% NaCl. Means and standard error of at least three biological replicates shown. Statistics calculated using a one-way ANOVA and Tukey-Kramer *post-hoc* test. ***, P-value <0.001.

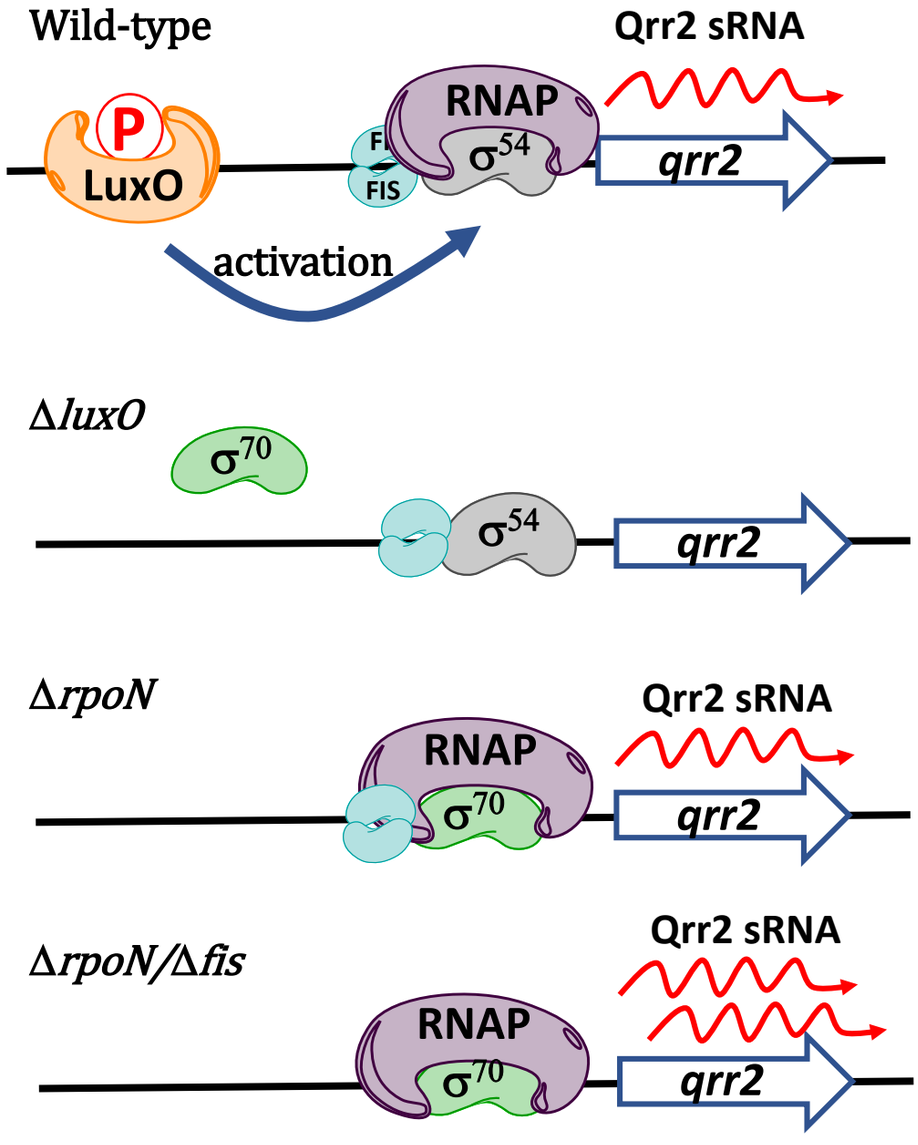

Figure 8: Model for *qrr2* transcription in the Δ*luxO* and Δ*rpoN* mutants. In the Δ*luxO* mutant, RpoN is bound to the *qrr2* -24 -12 promoter region, causing sigma-70 occlusion. We propose that in the absence of RpoN (sigma-54), RpoD (sigma-70) can bind to the *qrr2* -35 -10 promoter region to initiate transcription. Transcription by RpoD is increased further upon removal of Fis, as in the Δ*rpoN*/Δ*fis* mutant.